Supporting Information:

Significant promotion effect of carbon nanotubes on the electrocatalytic activity of supported Pd NPs for ethanol oxidation reaction of fuel cells: The role of inner tubes

Jin Zhang[1], Yi Cheng[1], Shanfu Lu[2], Lichao Jia[1], Pei Kang Shen[3] and San Ping Jiang[1,*]

[1]*Fuels and Energy Technology Institute & Department of Chemical Engineering, Curtin University, Perth, WA 6102, Australia*

[2]*School of Chemistry and Environment, Beihang University, Beijing 100191, China*

[3]*Advanced Energy Materials Research Laboratory, School of Physics and Engineering, Sun Yat-sen University, Guangzhou 510275, China*

*Corresponding author: Prof. San Ping Jiang (s.jiang@curtin.edu.au)

Experimental

Chemicals

CNTs samples with different number of walls were purchased from Nanostructrued & Amorphous Materials Inc., USA and were fabricated by catalytic chemical vapor deposition method. The CNTs were purified by ultrasonic treatment in 32 wt% HCl solution (Ajax Finechem) for 6 hours and then stirred at room temperature for 48 h before use. 5 wt% Nafion solution was purchased from DuPont Inc. Other chemicals including $PdCl_2$, tetrahydrofuran (THF), ethanol, were purchased from Sigma-Aldrich, and were used as received without further purifications. MilliQ water was used in the experiments.

Pd-CNTs Catalyst synthesis

CNTs were first functionalized by THF before the assembly of Pd NPs. In this method, 10 mg of $PdCl_2$ and 250 μL of 32 wt% HCl were added to 3mL of THF in 8 mL glass vial and were stirred at room temperature for several minutes until transparent brown solution was obtained. $[PdCl_4]^{2-}$ will be self-assembled to THF-CNTs via electrostatic attraction. The solids product was dried at 40 ^oC overnight, followed by heat-treatment in a tube furnace at 150 ^oC under 100 SCCM of H_2 for 2h to reduce $[PdCl_4]^{2-}$ to Pd NPs. The Pd-CNTs were collected and stored at vacuum desiccator. The Pd loading of synthesized Pd-CNTs catalysts was about 20 wt%, as determined by TGA.

Characterizations

The trace metal impurities in the CNTs after acid purification were analyzed by the Inductively Couple Plasma Optical Emission spectroscopy (ICP-OES, IRIS Intrepid II XSP,

Thermofisher). The CNTs were characterized by the Raman spectroscopy with excited wavelength of 1640 cm^{-1} (0.21 eV) and power density of 5 mW cm^{-2}. Morphologies of CNTs and Pd-CNTs were examined by transmission electron microscopy (TEM, JEOL 3000F) with operation voltage of 200 kV. The Brunauer-Emmett-Teller (BET) surface area and porosity of CNTs were investigated by Micromeritics Tristar II. The samples were first degassed at 150 ^oC for 24 h and then analyzed at 77 K. X-ray diffractometer (XRD) was used to obtain the crystal structures of Pd NPs with a Bruker D8 Advance Diffractometer (40 kV and 30 mA with Cu Kα 1.5406 Å). The thermogravimetric analysis of Pd-CNTs was performed by STD Q600, TA instrument under air atmosphere with air flow rate of 50 SCCM. X-ray photoelectron spectroscopy (XPS) measurements are conducted by using a ESCALAB 250 spectrometer with an Mg Kα radiator.

The electrocatalytic activity of as-synthesized Pd-CNTs catalyst as well as the pure CNTs was studied by cyclic voltammetry (CV) in 1.0 M KOH +1.0 M ethanol solutions. Catalyst electrodes were prepared by mixing the Pd-CNTs powder with 5.0 wt% Nafion solution. The mixture was sonicated at room temperature for 2 h before 10 μL catalyst ink was applied onto a glassy carbon disk (GCD) with a diameter of 7 mm. After solvent evaporation, a thin layer of catalyst with 0.05 mg cm^{-2} Pd loading was deposited on GCD surface to be employed as work electrode. The pure CNTs were deposited on the GCD surface with the same method of Pd-CNTs, and the CNTs loading was 0.026 mg cm^{-2}. A Pt plate and Hg/HgO (1.0 M KOH) electrode were used as the counter and reference electrodes, respectively. The polarization potential values in the text were converted based on RHE reference electrodes. All electrochemical tests were carried out on IVIUMSTAT potentiostat (Ivium technology, Netherland). Blank cyclic voltammetry tests were conducted in 1.0 M KOH solution. The stability of Pd-CNTs catalysts for ethanol oxidation reactions was evaluated, using chronoamperometry at 0.67 V (vs RHE) in 1.0 M KOH +1.0 M ethanol solutions.

Results and discussion

ICP, Raman spectroscopy and BET areas of CNTs

The as-received CNTs samples contain trace of impurities resulting from the catalytic CVD synthesis of CNTs. After purification, the amount of Fe, Co, Mo and Ni elements are substantially reduced to less than 0.5% as confirmed by the ICP-OES analysis (Table S1). The CNTs was then further examined by the TEM in terms of the morphology, wall numbers as well as the outer diameter distribution. The number of walls and outer diameter of CNTs were taken as average over more than 10 TEM images for each CNTs sample (Table S2).

Table S1 Concentration of impurities of CNTs after concentrated HCl treatment in ppm by ICP.

Samples	Co	Fe	Ni	Mo	Total, ×100ppm
CNTs-1	7	29	3	5	44
CNTs-2	57	23	3	27	100
CNTs-3	38	17	15	9	79
CNTs-4	-	21	20	1	42

Table S2 Outer diameter (OD), wall numbers of CNTs (n), I_D/I_G and BET surface area(S_{BET}), of CNTs samples after purification treatment.

Sample	Average OD/ nm	n	Average n	I_D/I_G	S_{BET}/ m^2g^{-1}
CNTs-1	1.97	1 (79%) 2 (16%) 3 (5%)	1	0.16	576.7
CNTs-2	3.80	2 (25%) 3 (52%) 4 (10%)	3	0.76	523.2
CNTs-3	7.45	5 (8%) 6 (20%) 7 (33.3%) 8 (20%) 9 (16.7%) 10 (10%)	7	1.35	538.8
CNTs-4	13.8	8 (9.5%) 10 (19%) 12 (38%) 14 (19%) 16 (14%)	12	2.50	270.6

Figure S1 is the Raman spectroscopy of CNTs measured at room temperature. The D band in 1281 cm^{-1} derives from the amorphous carbon and defects, while the G band in 1589 cm^{-1} indicates the graphite layer of CNTs.[1] The intensity ratio of defect-derived D band (I_D) to graphite-derived G band (I_G) reflects destructiveness of the SP^2 hybridized carbon atom.[2, 3] Thus, the increase of the I_D/I_G is an indication of the increased defect formation of the CNTs surface. I_D/I_G ratio is 0.16 for CNTs-1 (Fig.S1A), consistent that reported for SWNT.[4] In addition to the very small I_D/I_G ratio of 0.16, the presence of radial breathing modes (RBMs) also confirms the SWNT structure in CNTs-1.[5] In the case of CNTs-2, the ratio of RBMs intensity to D band intensity is higher than CNTs-1 (Fig.S1B), suggesting the reduction of SWNTs proportion in CNTs-2. The ratio of I_D/I_G increases with the increase of the wall numbers of CNTs and when the wall number increase to 12 in CNTs-4, the I_D/I_G ratio is 2.5.

Meanwhile, the absence RBMs and red-shift of D band in Fig.S1D shows that CNTs-4 is typical MWNTs. This indicates the lower crystallinity and consequently higher quantify of structural defects of CNTs-4 due to its multiple graphite layers,[6, 7] as compared to CNT-1, CNT-2 and CNT-3.

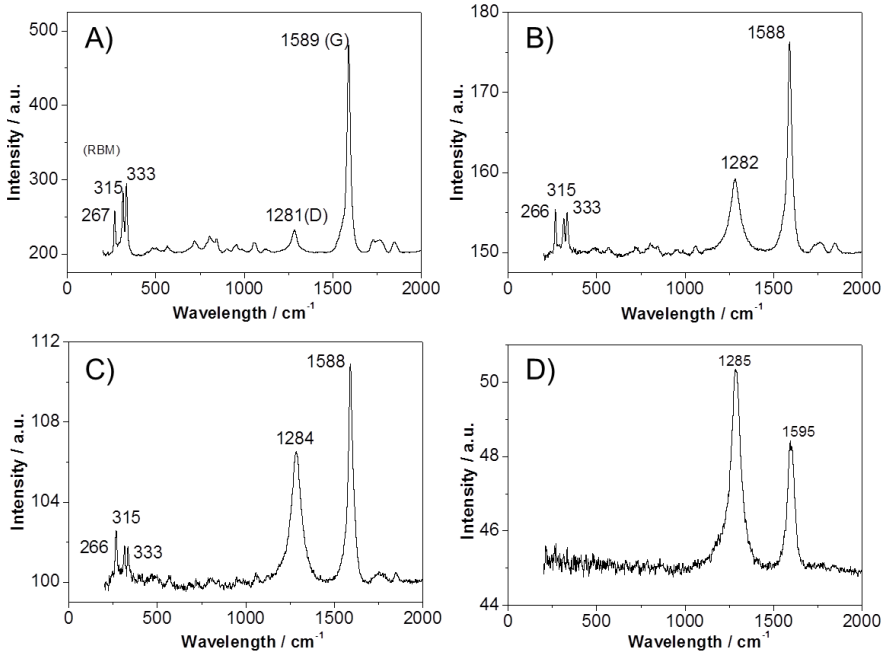

Fig. S1 Raman spectra of (A) CNTs-1, (B) CNTs-2, (C) CNTs-3 and (D) CNTs-4.

Based on the N_2 adsorption isotherms the BET surface area of CNTs-1, CNTs-2, CNTs-3 and CNTs-4 is 576.7, 523.2, 538.8 and 270.6 m^2 g^{-1}, respectively.

XPS

Fig.S2 is XPS spectra of Pd-CNTs NPs. XPS survey scan did not detect metal element impurities (Fig.S2C), indicating that the acid purification successfully removed the residual impurities of CNTs. The absence of Cl atoms also demonstrates that all the $[PdCl_4]^{2-}$ ions were reduced to Pd atoms by the H_2 reduction. Fig.S2A shows the XPS spectra of C 1s for four CNTs samples. Three peaks at 284.8 eV, 285.2 eV and 286.4 eV associate with carbon atoms in graphite-like walls, carbon defects that are attributed to C atoms no longer in the regular tubular structure[8] and high valence states C-O, respectively. Besides, the peak of 288.3 eV (–O-C=O), 289.0 eV (carbonates) presented in plasma treated CNTs are not detected in the CNTs samples,[8, 9] indicating the relative complete structure of CNTs. By the curve fitting, the percentage of oxygen-containing surface functional groups is 1.5%, 8.2%, 6.7% and 6.2% for CNTs-1, CNTs-2, CNTs-3 and CNTs-4, respectively. The Pd3d signals in the XPS spectra of Pd-CNTs consist of two pairs of doublets for $Pd3d_{3/2}$ and $Pd3d_{5/2}$

(Fig.S2B). In comparison with the standard spectra of metal Pd(0), the binding energy of $3d_{3/2}$ = 341.1 eV and $3d_{5/2}$ = 335.8 eV in Pd-CNTs are almost the same. Moreover, the high resolution Pd3d XPS reveals the positive shifts in the metallic Pd(0) peaks toward higher binding energy at 335.8 eV and 337.4 eV is assigned to the Pd(II) state in PdO or $Pd(OH)_2$. The binding energy and element distribution are given in Table S3. The content of oxidized Pd increases from 44.3 % to 67.3 % as the number of walls increases in the range of 1 to 12.

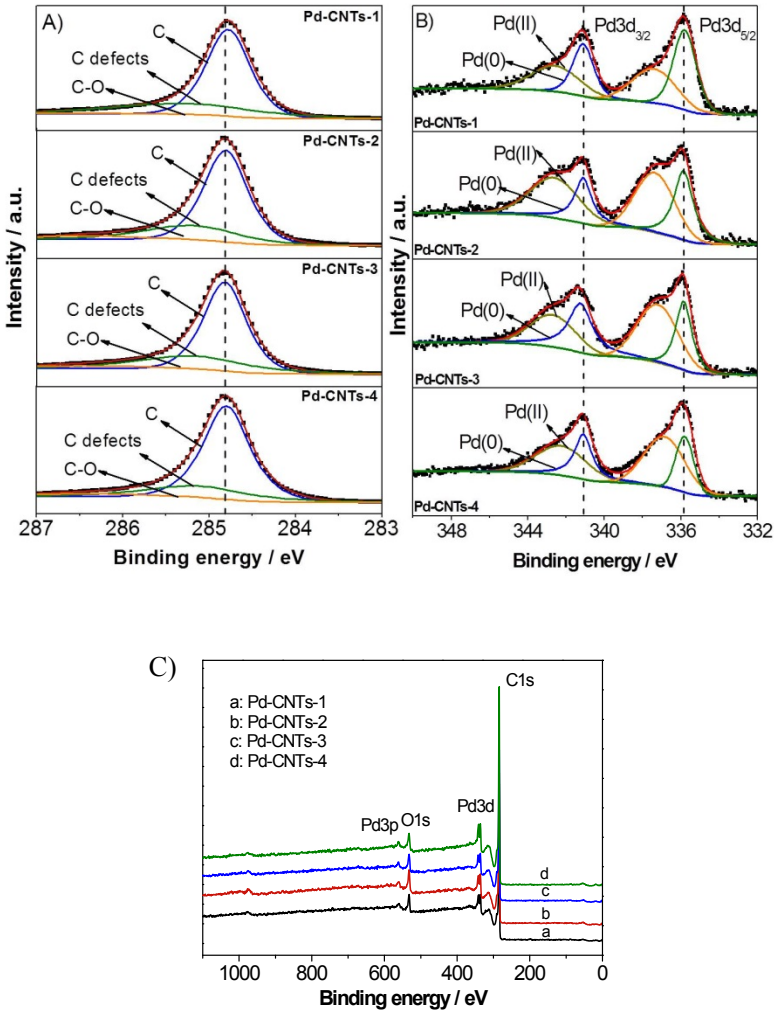

Fig.S2 C1s core XPS (A) and Pd 3d core level XPS(B) of Pd-CNTs. The XPS survey scan is shown in (C).

Table S3 XPS element state analysis, and binding energy of $Pd_3d_{5/2}$.

Sample	O/C	C-C,%	C-O,%	Ratio, %		Binding energy of $Pd3d_{5/2}$,eV	
				Pd(0)	Pd(II)	Pd(0)	Pd(II)
Pd-CNTs-1	4.5	70.7	1.5	55.7	44.3	335.8	337.4
Pd-CNTs-2	4.9	68.2	8.2	40.7	59.3	335.8	337.4

Pd-CNTs-3	4.4	66.7	6.7	35.2	64.8	335.8	337.2
Pd-CNTs-4	4.2	72.6	6.2	32.7	67.3	335.8	336.9

CV analysis of CNTs

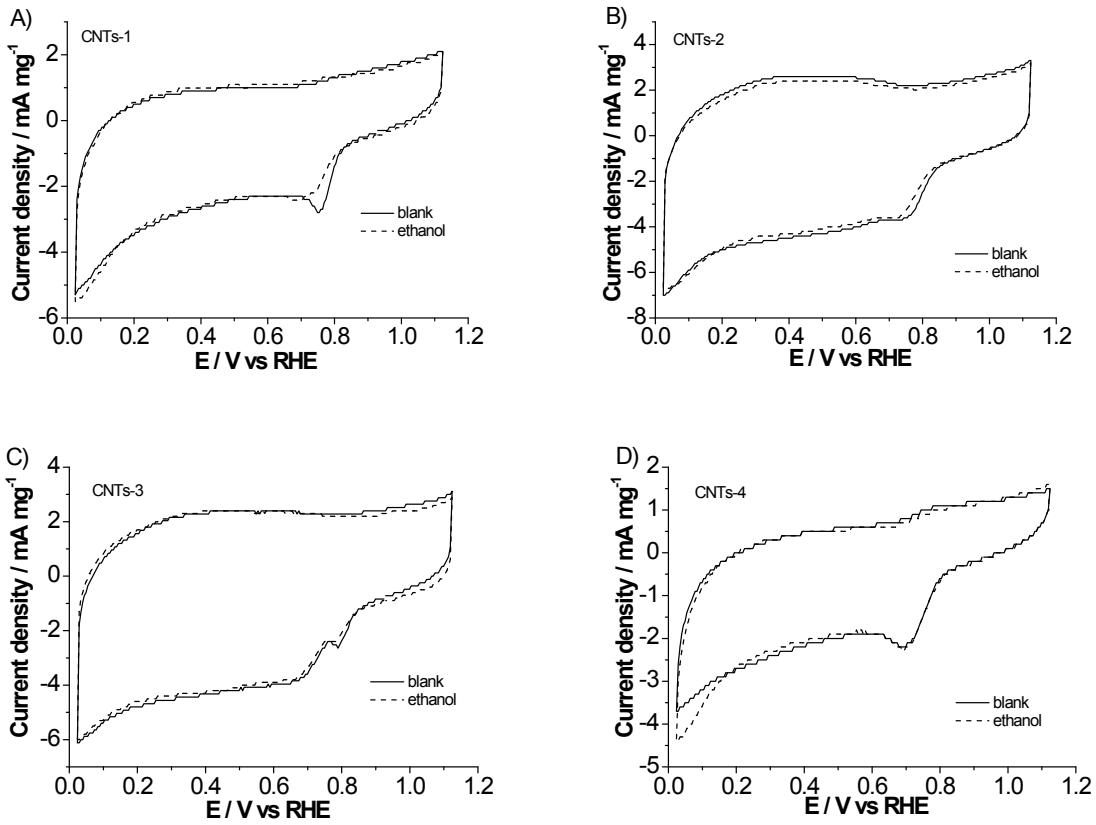

Fig.S3. Cyclic voltammetry of CNTs at different solution. Blank is measured in 1.0 M KOH solution, and ethanol is measured in 1.0 M ethanol in 1.0 M KOH solution. CNT loading was 0.026 mg cm^{-2} and scan rate was 100 mV/s.

The CV curves of CNTs at 1.0 M KOH solution and 1.0 M KOH and 1.0 M EtOH solutions are the same except the reduction peak of oxygen at around 0.8 V, which is due to the oxygen reduction reaction for the dissolved oxygen in the solution. That means that CNTs are inactive for the ethanol electrochemical oxidation. In other words, the defects and the metal impurities of CNTs do not contribute to the EOR process in alkaline solution.

References:

1. S. Osswald, E. Flahaut and Y. Gogotsi, *Chemistry of Materials*, 2006, **18**, 1525-1533.
2. I. D. Rosca, F. Watari, M. Uo and T. Akasaka, *Carbon*, 2005, **43**, 3124-3131.

3. Y. Cheng, C. Xu, L. Jia, J. Gale, L. Zhang, C. Liu, P. K. Shen and S. P. Jiang, *Applied Catalysis B: Environmental*, 2014, In Press.
4. V. M. Irurzun, M. P. Ruiz and D. E. Resasco, *Carbon*, 2010, **48**, 2873-2881.
5. R. Graupner, *Journal of Raman Spectroscopy*, 2007, **38**, 673-683.
6. A. M. Rao, S. Bandow, E. Richter and P. C. Eklund, *Thin Solid Films*, 1998, **331**, 141-147.
7. S. Costa, E. Borowiak-Palen, M. Kruszynska, A. Bachmatiuk and R. J. Kalenczuk, *Materials Science-Poland*, 2008, **26**, 433-441.
8. W. Sun, Z. Liu, C. Jiang, Y. Xue, W. Chu and X. Zhao, *Catalysis Today*, 2013, **212**, 206-214.
9. V. Datsyuk, M. Kalyva, K. Papagelis, J. Parthenios, D. Tasis, A. Siokou, I. Kallitsis and C. Galiotis, *Carbon*, 2008, **46**, 833-840.